

**PRECISION OF CEPHALOMETRIC LANDMARK IDENTIFICATION
3D Vs 2D**

by
Maritzabel Gubler

A thesis submitted to the faculty of the University of North Carolina at Chapel Hill in partial fulfillment of the requirements for the degree of Master of Science in the Department of Oral and Maxillofacial Radiology.

Chapel Hill
2008

Approved by:

Advisor: John B. Ludlow, D.D.S., M.S.

Reader: Andre Mol, D.D.S., M.S., Ph.D.

Reader: Lucia Cevidanes D.D.S., M.S., Ph.D.

© 2008

Maritzabel Gubler

ALL RIGHTS RESERVED

ABSTRACT

Maritzabel Gubler: Precision of Cephalometric Landmark identification 3D Vs 2D
(Under the direction of Dr. John Ludlow)

The purpose of this study was to determine if half-skull and multiplanar reconstruction (MPR) images derived from CBCT image volumes will provide more precise location of landmarks and measurements than conventional cephalometric radiographs.

A population of 20 pre-treated surgical orthodontic patients was radiographed and evaluated using lateral cephalometric and CBCT techniques. Four radiographic displays were used: conventional cephalogram, right and left half CBCT cephs, and MPR. Precision was calculated for 23 landmarks, 4 modalities and 20 cases using two measures of observer variation for identifying the same landmark in the same case and modality: ODM (Observers difference from the mean) and DEO (Difference from Every other Observer). Analysis of Variance (ANOVA) was computed for ODM or DEO for all modalities, landmarks, coordinates, and cases as every effect as well as all interactions among them. Statistical significance was defined as an α level of 0.05. Paired- t Tests were also used to assess each of the two calculations of variability for each landmark and the 6 possible combinations of 4 modalities. Bonferroni correction for multiple comparisons was applied and a p threshold of 0.0036 was calculated. Landmark variability clinically important used a threshold of 2mm.

Results indicate that overall statistically landmark variation was greater for conventional cephalogram than CBCT modalities when calculated using ODM and DEO approaches. The x and y overall modality variability were higher for conventional cephalograms than for any of the alternative modalities. Landmark variability over 2 mm was greater for conventional cephalogram for more than half of the landmarks. Only soft tissue Pogonion exceeded the 2mm for all modalities.

Based on the results of this study is possible to conclude that CBCT modalities provide a more precise location of landmarks overcoming problems obtained with conventional cephalograms.

To my family, who offered me unconditional love and support throughout the course of
my studies.

Also, this thesis is dedicated to Brian who has been a great source of happiness,
motivation and inspiration.

Finally, this thesis is dedicated to Cristina, my friend, sister and colleague without her I
would not be here at UNC.

ACKNOWLEDGEMENTS

Dr. John Ludlow (my mentor), for guiding me through every step of my thesis work, and for getting my ideas into focus during the process of my studies. Thank you for your patience, time and help.

Dr. Andre Mol, for making your explanations crystal clear, for your constructive comments, understanding and support.

Dr. Lucia Cevidanes, for your guidance, your decisive and energetic support during this project.

Dr. Ceib Phillips, and Dr. Se Hee Kim, for your invaluable assistance with the Statistical analysis.

Debbie Price, for your help and advice with software, and contribution to this project

Dr. Douglas Ford, for your help with the observation sessions and contribution to this project.

Dr. Enrique Platin, for providing encouragement, sound advice and constant support.

Dr. Donald Tyndall, for your kindness, openness, wisdom and contagious historic enthusiasm beyond the confines of radiology.

Mrs. Madge Webster, Sharon Green and Venecia Terry: for their friendship, sense of humor and for making a pleasant work environment during the clinics.

Mrs. Judy G. Dow, Mrs. Andrea Hall and Mrs. Tami Rice, for their kindness and constant assistance.

My Classmates and Friends: Kim Thaw, Wisam Al-Rawi. Abeer Alhadidi, Ginalyn Falconet for their friendship and company.

Dr. Cristina Maresca, for her friendship and company.

The UNC Oral and Maxillofacial Radiology Faculty, for guidance and support.

TABLE OF CONTENTS

	Page
ABSTRACT	iii
DEDICATION	v
ACKNOWLEDGEMENTS	vi
LIST OF TABLES	ix
LIST OF FIGURES	x
LIST OF ABBREVIATIONS.....	xii
A. Introduction.....	1
B. Materials and Methods.....	4
C. Results.....	10
D. Discussion.....	23
E. Conclusions.....	29
REFERENCES	30

LIST OF TABLES

Table		Page
Table 1	Landmarks selection and definition	18
Table 2	ANOVA-Test Effects DEO	11
Table 3	ANOVA-Test Effects ODM	11
Table 4	Mean modality variation – average of variation in landmark identification for all landmarks	12
Table 5	Paired T-Tests of landmark identification –average observer variation from mean (ODM) for 4 cephalometric modalities	12
Table 6	Paired T-Tests of landmark identification –average observer variation from every other observer (DEO) for 4 cephalometric modalities	12
Table 7	Paired comparisons of DEO landmark variation for Conventional and CBCT views by Landmark for x and y deviations.....	21
Table 8	Paired comparisons of DEO landmark variation for CBCT views by Landmark for x and y deviations	22
Table 9	X and y landmark identification variability by modality	23

LIST OF FIGURES

Figure		Page
Figure 1	Vertical orientation.....	5
Figure 2	Rotation sagittal plane.....	5
Figure 3	Horizontal orientation.....	5
Figure 4	Landmark identification variation for conventional cephalogram, average of x and y deviation for each landmark. Difference in landmark variability when using ODM or DEO.....	15
Figure 5	Landmark identification variation for Left CBCT, average of x and y deviation for each landmark. Difference in landmark variability when using ODM or DEO.....	15
Figure 6	Landmark identification variation for MPR, average of x and y deviation for each landmark. Difference in landmark variability when using ODM or DEO.....	16
Figure 7	Landmark identification variation for Right CBCT, average of x and y deviation for each landmark. Difference in landmark variability when using ODM or DEO.....	16
Figure 8	Landmark identification x and y, DEO variability in conventional cephalograms, x = anterior-posterior direction, y = caudal-cranial direction.....	17
Figure 9	Landmark identification x and y, DEO variability in MPR, x = anterior-posterior direction, y = caudal-cranial direction.....	18
Figure 10	Landmark identification x and y, DEO variability in Left CBCT, x = anterior-posterior direction, y = caudal-cranial direction.....	18
Figure 11	Landmark identification x and y DEO variability in Right CBCT, x = anterior-posterior direction, y = caudal-cranial direction.....	19

Figure 12	Nasion identification when Sella is the origin of matrix, DEO variability.....	19
Figure 13	Nasion identification when Sella is replaced by a tick mark on the ruler, DEO variability.....	20

LIST OF ABBREVIATIONS

CBCT	Cone Beam Computed Tomography
DEO	Difference for every observer
ICRP:	International Commission On Radiological Protection
FOV:	Field Of View
mm	Millimeter
MPR	Multiplanar Reconstruction
ODM	Observer Difference from the Mean
PA	Posterioranterior cephalograms
SD	Standard deviation
2D	Two Dimensional
3D	Three Dimensional

INTRODUCTION

With the availability of Cone Beam Computed Tomography (CBCT) for orthodontic diagnosis it is theoretically possible to use volumetric data to obtain more accurate skeletal measurements; therefore the problems noted with conventional cephalograms can be avoided such as: errors in patient position, differential magnification on bilateral structures, superimposition of craniofacial structures, and the presence of asymmetry that further complicate the localization of bilateral structures. (Midtgard et al., 1974; Houston 1983) The previous standard in craniofacial and orthognatic surgical planning and monitoring using the lateral cephalogram is still popular and has been sustained by its ease of reproducibility and low cost. (Por et al., 2005) However, the disadvantage of this technique is that it requires multiple angle measurements to assess the direction of movement of a landmark. Nevertheless, it is difficult to make judgments about the complex relationships of the facial bones by measuring only a series of angles projected onto two-dimensional radiographs. Second, conventional two-dimensional cephalometry projects three-dimensional structures into two-dimensions. Thus, it is difficult to directly compare lengths and angles for assessment of treatment effects and for planning treatment. (Hideki et al., 2000) Furthermore, due to inherent geometric magnification, distortion, and superimposition of the craniofacial structures on the cephalometric radiograph, a reliable and accurate evaluation of these structures in patients with severe

anomalies such as craniofacial syndromes is difficult. Three-dimensional (3D) computed tomography (CT) avoids anatomic superimposition and problems due to magnification and offers the opportunity to evaluate the craniofacial structures from unobstructed perspectives and with less distortion than the two-dimensional method. (Papadopoulos et al., 2000) CBCT characteristics are well suited for imaging the craniofacial area. This technology provides clear images of highly contrasted structures and is extremely useful for evaluating bone. The CBCT scanner can collect volume data by means of a single rotation (360°-720°), taking a scanning time between (10-70 seconds) (Scarfe et al., 2006). These scanners use a cone beam geometry, which permits a more efficient utilization of x-ray photons. The dose of cone beam computed tomography (CBCT) is relatively low; published reports indicate that the effective dose of radiation (average range 36.9-50.3 microsievert) is significantly reduced by up to 98% compared with “conventional” fan-beam CT systems. (Cohnen et al., 2002; Schulze et al., 2004; Ludlow et al., 2003; Ngan et al., 2003; Ludlow et al., 2006). CBCT systems offer images with a high spatial resolution both longitudinally and axially through employment of an isotropic voxel matrix; this produces sub-millimetre resolution ranging from 0.4 mm to as low as 0.125 mm. (Yajima et al., 2006; Scarfe et al., 2006). Some CBCT scanners provide large fields of view (9-12 inch), which allow 3D reconstruction and visualization of the full maxillofacial region. In addition, CBCT allows the creation of conventional views from the image volume, including panoramic, lateral and antero-posterior views. The value of CBCT imaging in implant planning, surgical assessment of pathology, TMJ assessment and pre and postoperative assessment of craniofacial structures has been reported. (Honda et al., 2004; Tsiklakis et al., 2004; Honda et al., 2004) For these reasons, three-

dimensional computed tomography has found increasingly widespread use in maxillofacial surgery and orthodontics for a variety of clinical and research purposes (Hideki et al., 2000).

Traditionally lateral and frontal cephalometric radiographs have been used to determine craniofacial discrepancies or deformities, with the analysis being based on a series of cephalometric points. The evaluation of these radiographs may be difficult due to overlapping anatomical structures and the differential magnification of lateral structures which results in distortion. (Bergersen, 1980) There have been reports of inaccuracies and poor precision in reproducing these cephalometric points. (Midtgard et al., 1974; Houston, 1983; Kantor et al., 1993)The use of CBCT instead of conventional cephalograms provides an alternative method for assessment of craniofacial relationships of selected orthodontic and surgical patients.

This study attempts to determine if half-skull and multiplanar reconstruction (MPR) images derived from CBCT image volumes will provide more precise location of landmarks and measurements than conventional cephalometric radiographs.

The specific aim was to test the null hypothesis that the precision of landmark localization is not different for CBCT half-skull projections, MPR displays, and conventional cephalograms in a sample of pre-treatment surgical orthodontic patients.

MATERIALS AND METHODS.

With Institutional Review Board approval, a sample of 20 subjects from a population of pre-treated surgical orthodontic patients (grant # NDCR DE 00521526) at the University of North Carolina School of Dentistry were radiographed using lateral cephalometric and CBCT techniques which were evaluated using four radiographic displays: conventional cephalograms, right and left half CBCT skull projections and MPR views with surfaced rendered CBCT volumes.

Image acquisition.

Conventional cephalograms were acquired by positioning the patient in natural head position, stabilized by cephalostat ear rods inserted into the external auditory meati. The source-midsagittal plane distance was 152.4 cm (5 feet). A photostimulable phosphor plate was used as the detector and positioned 11.5 cm from the midsagittal plane. The plate was scanned and digitized at 300 dpi and 16 bits (Digora PCT, Soredex, USA). CBCT volumes were acquired using a NewTom 3G (QR-NIM s.r.l., Verona, Italy). A 12 inch receptor field was used to include the entire facial anatomy for cephalometric purposes. The “large field” and “high resolution” options were selected for primary image reconstruction. The secondary study data was generated with 0.4mm axial slice thicknesses and isotropic voxels. The axial images were exported in DICOM format and imported in Dolphin 3D (version 10.5, Dolphin Imaging & Management Systems, Chatsworth, CA). To obtain diagnostically suitable images three steps were required using the Dolphin software. First, segmentation was performed for soft and hard tissue where manipulation of the histogram limits the data that is displayed. This step is performed to reduce noise that could affect the image quality. After segmentation the data

was reoriented to approximate the orientation of a conventional cephalometric image. Using the coronal view, the volume was rotated until the transporionic line of the data was oriented horizontally [figure 1]. Using the axial view, the volume was rotated until the midsagittal plane of the data was oriented vertically [figure 2]. Using the sagittal view, the volume was rotated until the Frankfort plane of the data was oriented horizontally [figure 3]. Next, lateral radiographs were built from the reoriented data, using partial volumes (right and left side) to create cephalometric projections of separate halves of the skull. The radiographs were created using parallel ray projections (orthogonal) perpendicular to the midsagittal plane. Resulting images from CBCT volumes had 0% (1:1) magnification. Dolphin imaging software (version 10.5) was used for cephalometric landmark location of 3D images.

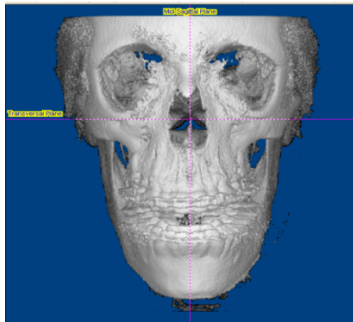


Figure 1. Vertical orientation

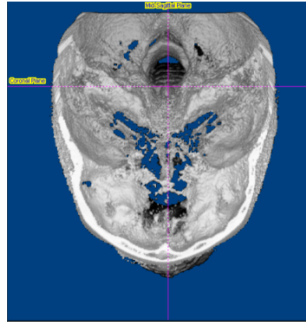


Figure 2. Rotation sagittal plane

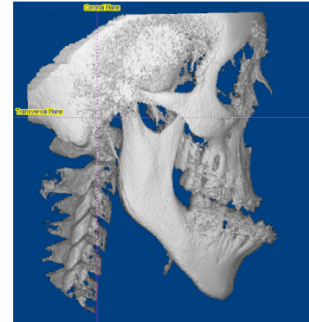


Figure 3. Horizontal orientation

Matrix generation

MPR images generated by NewTom 3G produced a signal gray scale of 12 bit with an acquisition matrix of 1024 x 1024, a voxel size of 0.25 mm and a spatial resolution of 1.4 (line pair mm). The matrix size of the exported right and left half skull projections was 512 x 512, producing a 205 Kilobyte JPEG image. Based in the coordinate system, the matrix was established for 3D and 2D modalities. A 3D virtual model was created

from the study and used to determine head orientation and the center of the 3D coordinate system. Using lateral frontal and superior views, coronal and sagittal views of the 3D head rendering, the midsagittal plane of the model was oriented vertically, the transporionic line was oriented horizontally and Frankfort horizontal plane was oriented horizontally. The center of the coordinate system was determined by the intersection of the transporionic line and the midsagittal plane (Kumar et al., 2008). Coordinates system(x, y) corresponded to right and left half skull CBCT projections and conventional cephalograms where the origin was set at “sella” (0, 0). Accordingly to the software description, it was possible to use the same origin (sella) of the coordinate system for 3D and 2D, if (z, y) was used in 3D, equivalent to the (x, y) coordinates in 2D. This approach could not be followed for the difficulty of visualization of Sella in the half skull projections. Therefore it was decided to replace Sella for an easy identifiable landmark such as a tick mark at the ruler, of the half skull projections and conventional cephalograms.

Image display.

Different image modalities were displayed on one of two computer workstations. The first station was designated for MPR views. The second station was assigned for the remaining modalities (right and left half skull projections and conventional cephalograms). Left skull projections were reorientation using the “mirror” tool, to permit digitizing of the landmarks in the same reference matrix

Determination of Landmarks.

The landmarks listed in Table 1 were evaluated in this study. The measurements were selected to include both vertical and antero-posterior components of the craniofacial

structures. The landmarks represented both the midsagittal and bilateral anatomical structures with different degrees of identification difficulty. For the calculation of the magnification for conventional cephalograms, the distance between the source and the midsagittal plane in the cephalostat was measured as 5 feet (152.4 cm). The distance between the receptor and the midsagittal distance was 11.5 cm. Thus,

$$\text{Percent magnification} = 11.5/152.4 \times 100\% = 7.5\%$$

Based on this magnification factor, conventional images were calibrated prior to landmark identification by each observer. This was done by clicking on points at 0 and 40 mm of the radiographic image of an aluminum ruler included in the midsagittal plane of each cephalometric image. The dimension for this measured distance was input as 43.0 mm to account for the 7.5% magnification at the midsagittal plane. Because half skull modalities were projected at 1:1, observers identified 2 points 40.0 mm apart on the electronic ruler included in the border of Dolphin images and input this measure as 40 mm to calibrate the software measurement tool.

Observations sessions.

All 80 images (20 patients per modality) were evaluated by 5 observers. Two observers were experienced oral and maxillofacial radiologists; one was a third year radiology resident; one was an experienced orthodontist; and one was a second year orthodontic resident. Before the viewing sessions, each observer received instructions and was trained on the use of the different modalities. During digitizing of the landmarks, the observers viewed modalities separately in an alternating order. They viewed 10 patients per week in two different sessions. The observers were allowed to use enhancement tools such as magnification, brightness, and contrast to improve the visualization of the

landmarks. After the observers digitized all the landmarks, the landmark coordinates were imported into Excel (Microsoft, Cupertino, CA) for assessment of precision

Analysis.

Precision was calculated for 23 landmarks, four modalities, and 20 cases using 2 formulas. The first formula calculated average observer difference from the mean (ODM) First the mean x and y coordinate was calculated using the 5 observers location of the same landmark on the same image. Then the absolute value of the difference of each observer's point location from the mean was calculated. Finally the average of all observers' absolute difference from the mean was determined. The second formula for determining observer variability utilized the average of all combinations of the absolute value of the difference of one observer from another or the difference for every observer (DEO).

Analysis of Variance was computed for ODM or DEO as outcome variables and Modality, Landmark, Coordinate, and Case as principle effects as well as all of the first order interactions of these effects in the ANOVA model. An alpha level of 0.05 was established as the level for statistical significance. Paired- t Tests were also used to assess each of the two calculations of variability for each landmark and the 6 possible combinations of 4 modalities. Because multiple landmarks and modalities were investigated, the risk of a type II error is increased. A Bonferroni correction for multiple comparisons ($6 \times 23 = 138$) was applied and a p threshold of 0.00036 for an alpha level of 0.05 was calculated ($\alpha/n = 0.05/138$). Landmark variability of potential clinical importance is reported using a threshold of 2 mm.

TABLE 1. Landmarks selection and definition.

LANDMARK	DEFINITION
Ruler Point 1	One of the points necessary to calibrate the size of this image. Accuracy in location of This point determines the accuracy of your final measurements (Click on ruler at tick mark 100 in the Sagittal plane).
Ruler Point 2	One of the points necessary to calibrate the size of this image. Accuracy in location of this point determines the accuracy of your final measurements (Click on ruler at tick mark 60 in the Sagittal plane).
Tip of the Nose	Pronasale, point of the anterior curve of the nose.
Subnasale	Point where the nose connects to the center of the upper lip.
Soft Tissue A point	The most concave point between subnasale and the anterior point of the upper lip.
Upper Lip	Most anterior point on the curve of the upper lip.
Stomion superius	Most inferior point on the curve of the upper lip.
Stomion inferius	Most superior point on the curve of the lower lip.
Lower Lip	Most anterior point on the curve of the lower lip.
Soft tissue B point	Most concave point between the lower lip and the soft tissue chin.
Soft tissue Pogonion	Point on the anterior curve of the soft tissue chin.
Soft tissue Gnathion	The midpoint between the most anterior and inferior points of the soft tissue chin in the midsagittal plane.
Nasion	Intersection of the internasal suture with the nasofrontal suture in the midsagittal plane.
Orbitale	Lowest point of the floor of the right orbit, the most inferior point of the external border of the orbital cavity.
Sella	Center of the pituitary fossa of the sphenoid bone.
Condylion	The most posterior superior point of the right condyle.
ANS	The tip of the anterior nasal spine.
A point	Deepest point of the curve of the maxilla, between anterior nasal spine and the dental alveolus.
Upper incisor tip	Incisal tip of the right upper central incisor.
Menton	Most inferior point of the symphysis.
Anatomical Gnathion	Midpoint between the most anterior and inferior point on the bony chin.
Pogonion	Most anterior point on the midsagittal symphysis.
B point	Most posterior point in the concavity along the anterior border of the symphysis.
Lower incisor tip.	Tip of the right lower central incisor.
Gonion	Location depends of the analysis. 1. The most convex point along the inferior border of the right ramus. 2. The most convex point where the posterior inferior curve of the right ramus and ascending ramus meet.

RESULTS

Overall modality variation

Tables 2 and 3 show the Analysis of Variance (ANOVA) for ODM (Observer Difference from the Mean) and DEO (Difference of each observer from Every other Observer) respectively by all modalities, landmarks, coordinates and cases. Every effect and the primary interactions among them, show a statistically significant difference. Table 4 presents average variation in landmark identification for all landmarks by modality variation calculation. DEO was consistently greater than ODM. Table 5 shows the Paired T-Test results for ODM pooling all landmarks for the 6 combinations of modalities. There was statistically greater observer variation for conventional cephalometric landmark identification than MPR and half skull projection CBCT views ($p < 0.0001$). MPR and half skull projection CBCT views were not statistically different from each other ($p > 0.05$). Table 6 presents the same pattern of statistically significant results for DEO as was seen when variation was calculated as ODM.

TABLE 2. ANOVA-Test Effects DEO

Source	DF	Sum of Squares	F Ratio	Prob> F
Modality	3	406.8	233.4	<.0001
Landmark	22	103.2	81.2	<.0001
Coordinate	1	18.3	31.4	<.0001
Case	19	329.0	29.8	<.0001
Modality*Landmark	66	323.2	8.4	<.0001
Modality*Coord	3	92.8	53.2	<.0001
Modality*Case	57	560.1	17.0	<.0001
Landmark*Coord	22	430.1	33.6	<.0001
Landmark*Case	418	625.0	2.6	<.0001
Coordinate*Case	19	36.1	3.2	<.0001

TABLE 3. ANOVA-Test Effects ODM

Source	DF	Sum of Squares	F Ratio	Prob> F
Modality	3	175.3	228.3	<.0001
Landmark	22	424.1	75.3	<.0001
Coordinate	1	6.4	24.9	<.0001
Case	19	142.1	29.2	<.0001
Modality*Landmark	66	133.7	7.9	<.0001
Modality*Coord	3	40.14	52.3	<.0001
Modality*Case	57	256.6	17.6	<.0001
Landmark*Coord	22	175.0	31.1	<.0001
Landmark*Case	418	263.2	2.5	<.0001
Coordinate*Case	19	18.3	3.8	<.0001

TABLE 4. Mean modality variation- average of variation in landmark identification for all landmarks

Modality Variability Calculation	Conventional	MPR	Right half CBCT	Left half CBCT
DEO	2.13	1.31	1.41	1.39
ODM	1.38	0.85	0.90	0.88
DEO/ODM %	154%	154%	157%	158%

TABLE 5. Paired T-Tests of landmark identification –average observer variation from mean (ODM) for 4 cephalometric modalities

	MPR- Conventional	Right CBCT- Conventional	Left CBCT- Conventional	Right CBCT- MPR	Left CBCT- MPR	Left CBCT- Right CBCT
Mean Difference	-0.53	-0.48	-0.50	0.05	0.03	-0.02
Std Error	-0.53	-0.48	-0.50	0.005	0.005	0.003
Prob> t	<.0001	<.0001	<.0001	0.2726	0.5181	0.5659

TABLE 6. Paired T-Tests of landmark identification –average observer variation from every other observer (DEO) for 4 cephalometric modalities

	MPR- Conventional	Right CBCT- Conventional	Left CBCT- Conventional	Right CBCT- MPR	Left CBCT- MPR	Left CBCT- Right CBCT
Mean Difference	-0.82	-0.72	-0.75	0.10	0.08	-0.03
Std Error	0.11	0.11	0.15	0.008	0.008	0.05
Prob> t	<.0001	<.0001	<.0001	0.2044	0.3799	0.6166

Landmark variation

Landmark identification variation, averaging x and y deviation for each landmark and each modality is seen in figures 4-7. These figures also illustrate the difference in the magnitude of landmark variability when calculated using ODM or DEO approaches. In general DEO calculations are about half again as large as ODM calculations of landmark variability. Within modalities, patterns of variability differed with conventional cephalometric landmark patterns differing from CBCT patterns. Identification of Condylion, Gonion, Porion as well as Soft tissue Pogonion exhibited greatest variability in conventional cephalograms. While none of the landmarks exhibited ODM variability over 2 mm for the alternate modalities, soft tissue pogonion was generally more variable than other landmarks. Applying the more stringent measure of variability measurement, Gnathion, A Point, Lower Stomion, B Point, Menton, Pogonion, Soft tissue B point, Orbitale, Soft tissue Gnathion, Condylion, Soft tissue Pogonion, Gonion, and Porion each exceeded the 2 mm threshold of DEO variability for conventional cephalograms. Of these landmarks, only Soft tissue Pogonion exhibited variability exceeding 2 mm for all other modalities. Soft tissue Gnathion and Condylion also exceeded 2 mm for Right half CBCT.

The x and y contributions to overall modality variability can be seen in Table 9. Both x and y variability were higher for conventional cephalograms than for any of the alternative modalities. While x variation was greater than y variation for conventional cephalograms, this pattern was reversed with y variation being greater than x for CBCT modalities. Landmark identification variation, isolating x and y deviation for each landmark and each modality is seen in figures 8-11. Anterio-posterior DEO variability (x)

exceeding 2 mm was seen in conventional cephalograms for A Pt, Soft Tissue B Point, B Point, Gnathion, Pogonion, Soft Tissue Gnathion, Orbitale, Condylion, Lower Stomion, Soft Tissue Pogonion, Menton, Porion, and Gonion. For Right CBCT views, DEO x variation greater than 2 mm was seen with Gonion and Lower Stomion. For MPR views only Orbitale exhibited greater than 2 mm x variation. No landmarks exceeded 2 mm of x variability for Left CBCT views.

Calculation of the variability of Nasion using DEO approach demonstrated that when the origin for x and y matrix was established at Sella from the original data, Nasion exhibited greater variability for Right and Left CBCT views compared with conventional cephalograms (Figure 12). Nasion identification variation for Right, Left CBCT views and conventional shows a lower variability when Sella was replaced for a tick mark on the ruler (Figure 13).

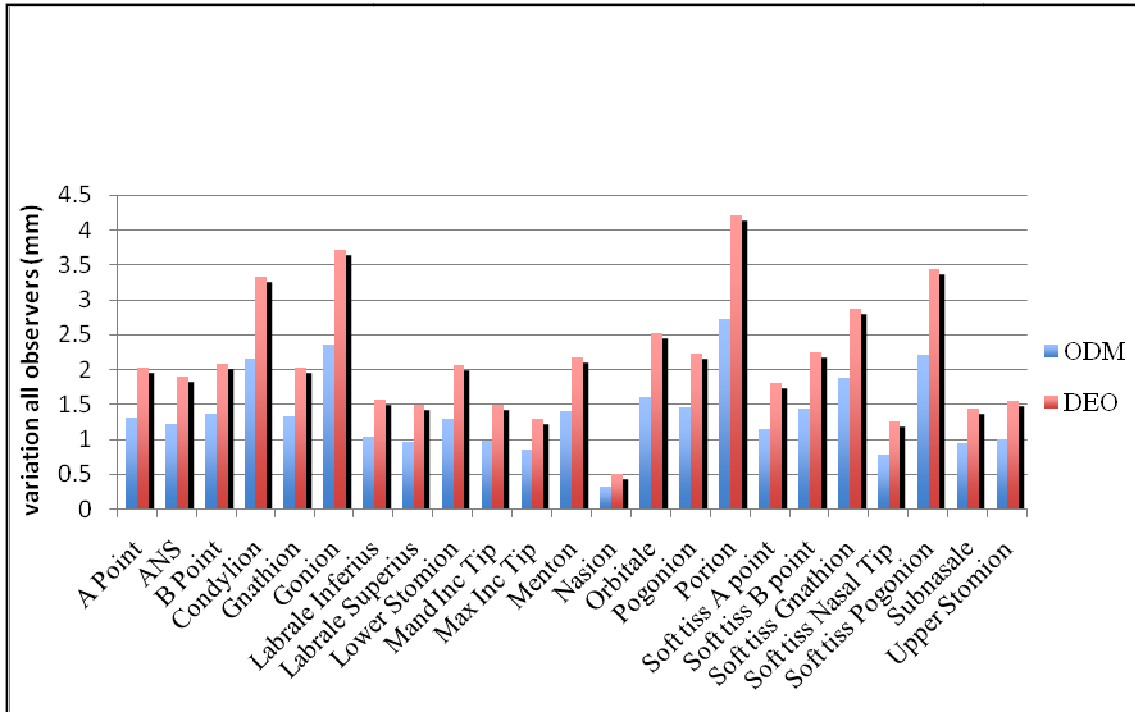


Figure 4. Landmark identification variation for conventional cephalogram, average of x and y deviation for each landmark. Difference in landmark variability when using ODM or DEO.

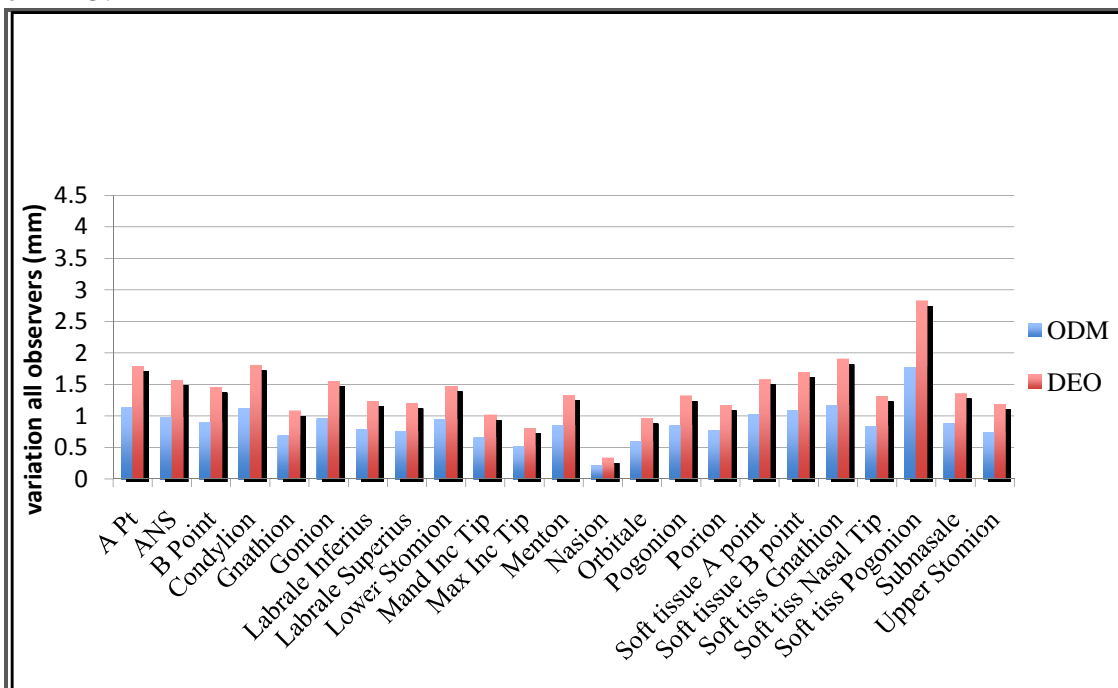


Figure 5. Landmark identification variation for Left CBCT, average of x and y deviation for each landmark. Difference in landmark variability when using ODM or DEO.

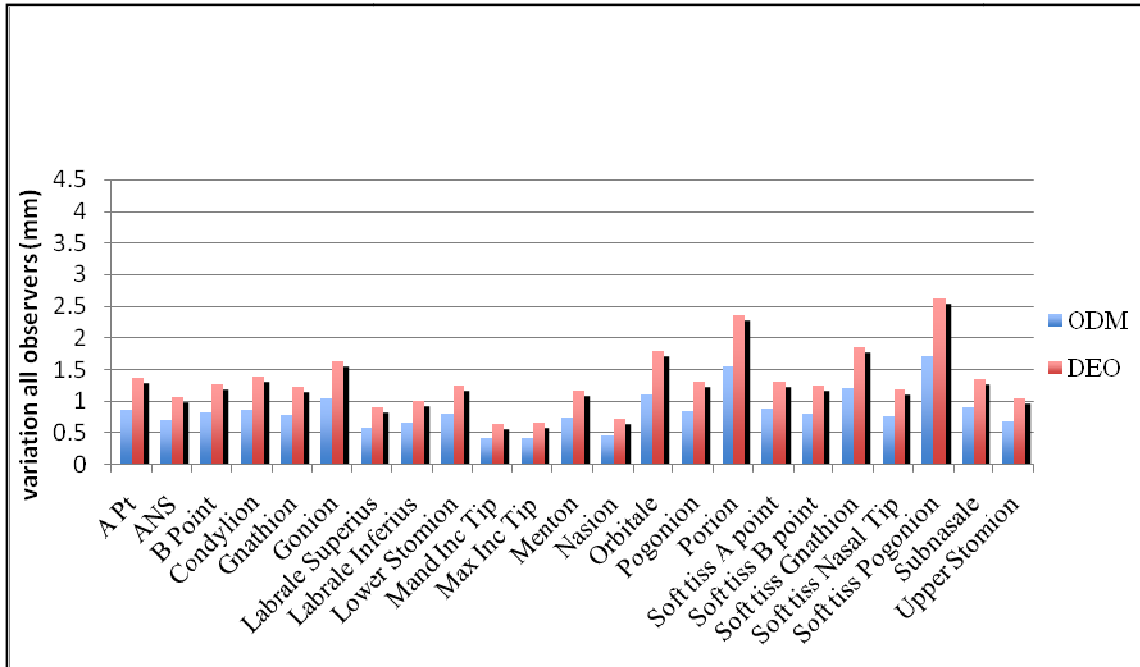


Figure 6. Landmark identification variation for MPR, average of x and y deviation for each landmark. Difference in landmark variability when using ODM or DEO.

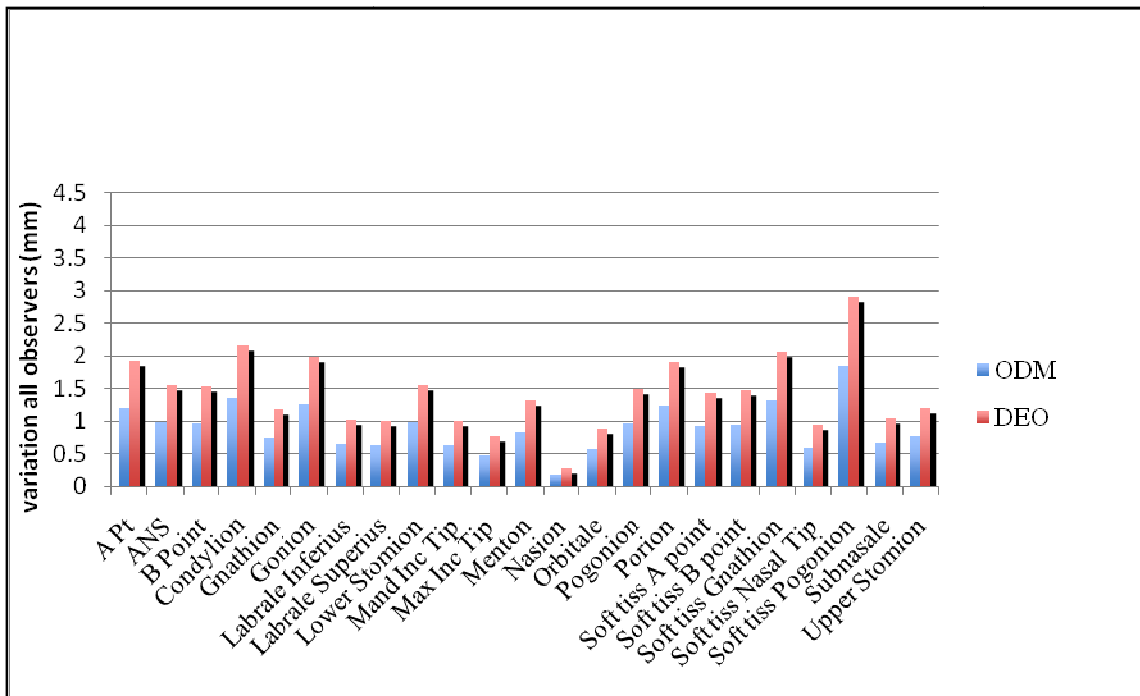


Figure 7. Landmark identification variation for Right CBCT, average of x and y deviation for each landmark. Difference in landmark variability when using ODM or DEO.

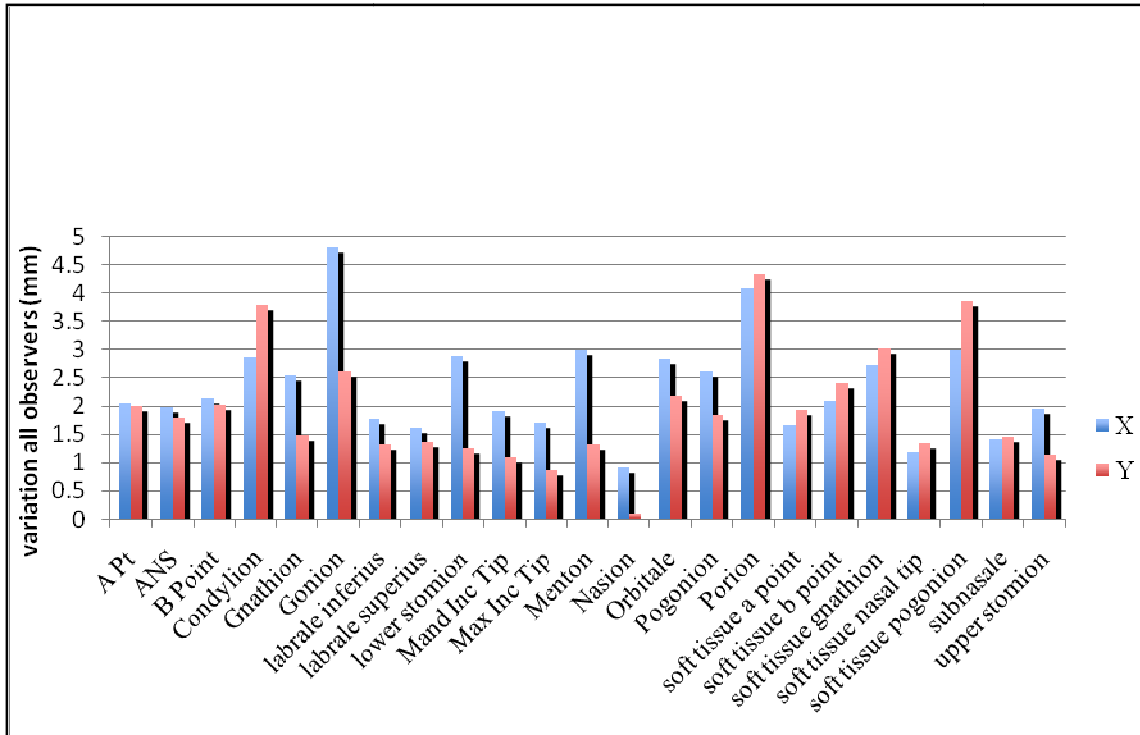


Figure 8. Landmark identification x and y, DEO variability in conventional cephalograms, x = anterior-posterior direction, y = caudal-cranial direction

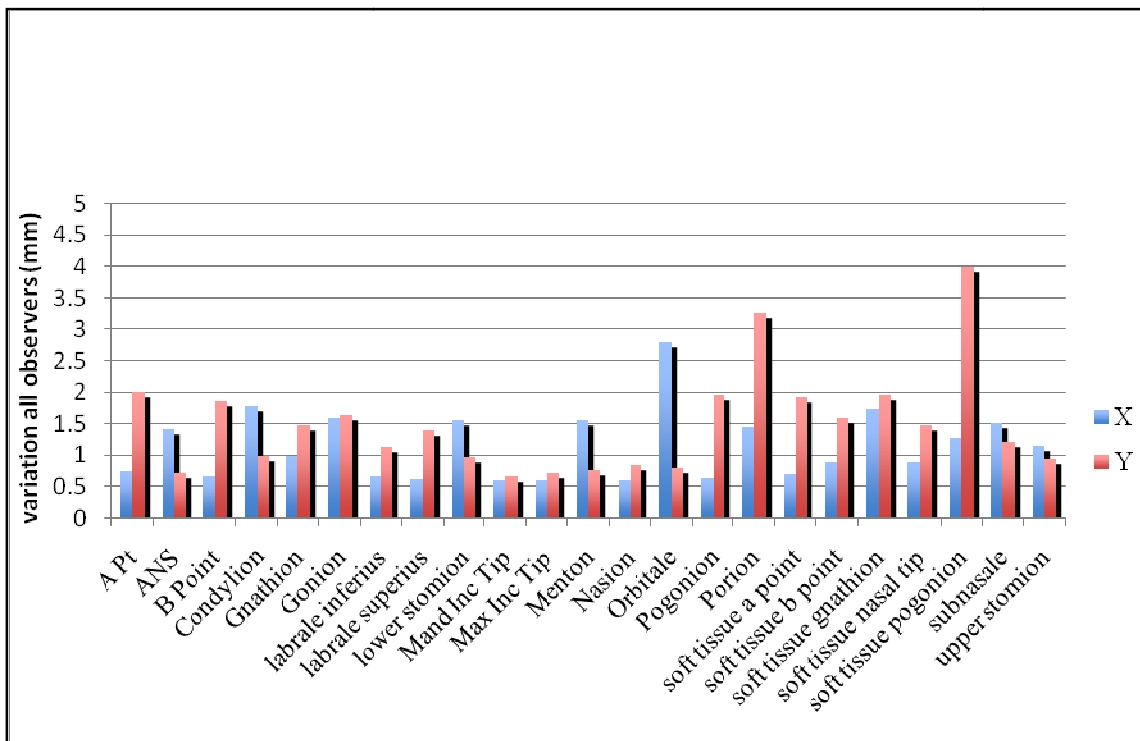


Figure 9. Landmark identification x and y, DEO variability in MPR, x = anterior-posterior direction, y = caudal-cranial direction

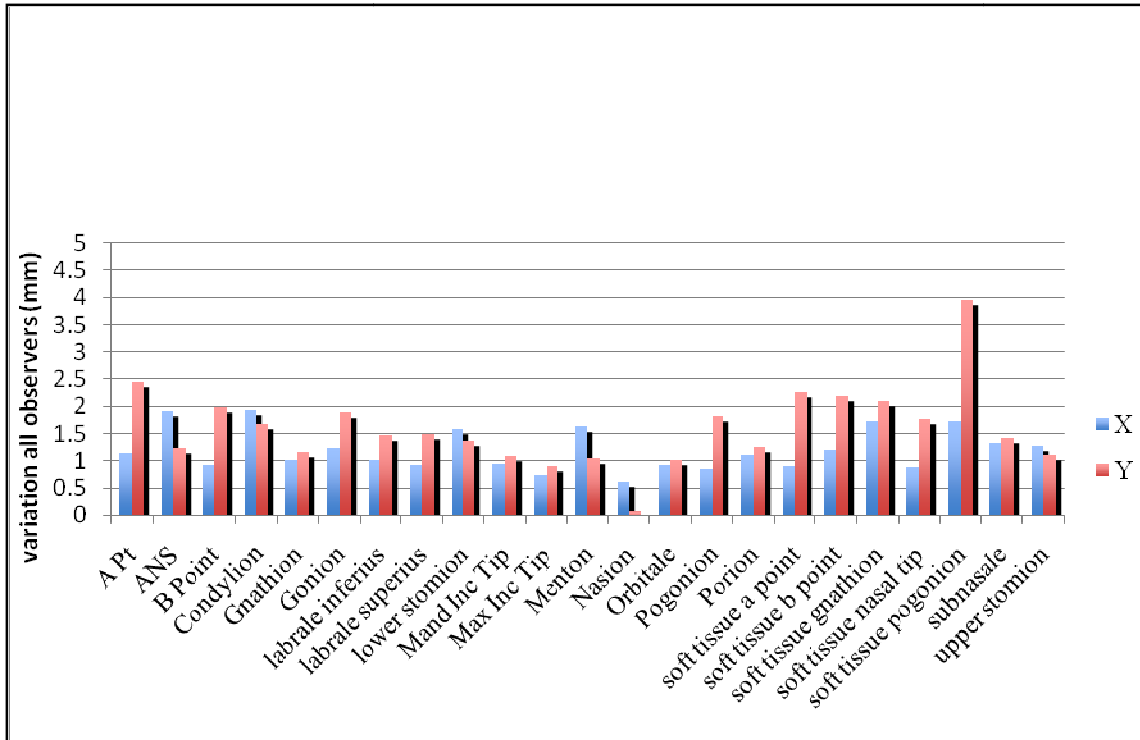


Figure 10. Landmark identification x and y, DEO variability in Left CBCT, x = anterior-posterior direction, y = caudal-cranial direction

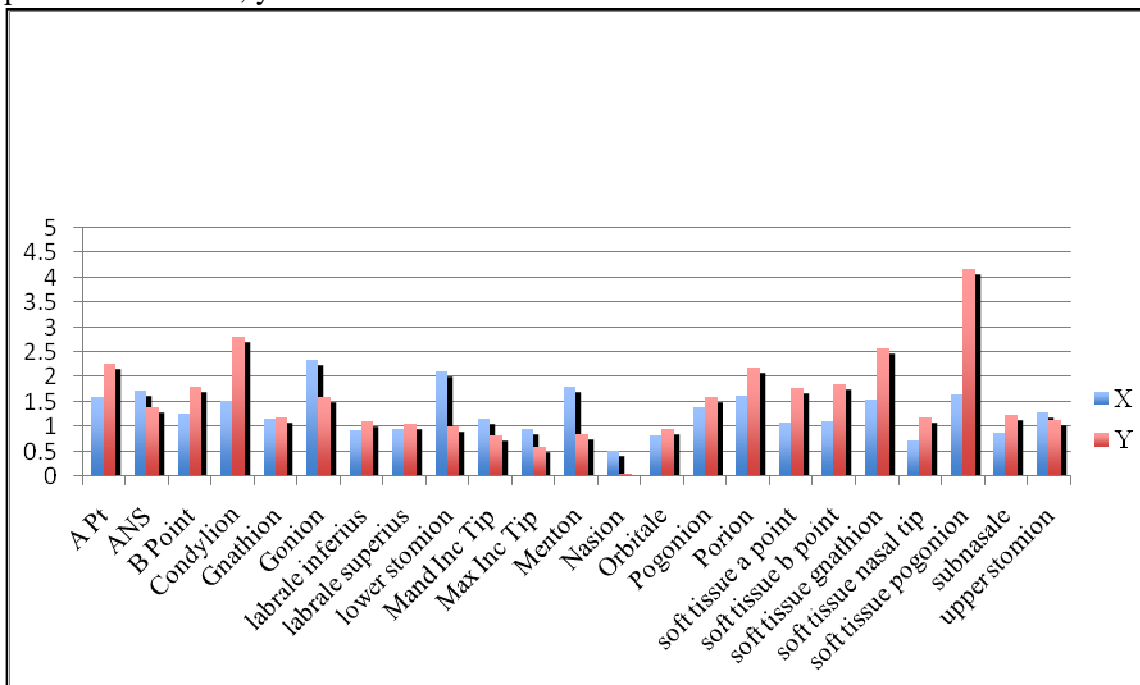


Figure 11. Landmark identification x and y DEO variability on in Right CBCT, x = anterior-posterior direction, y = caudal-cranial direction.

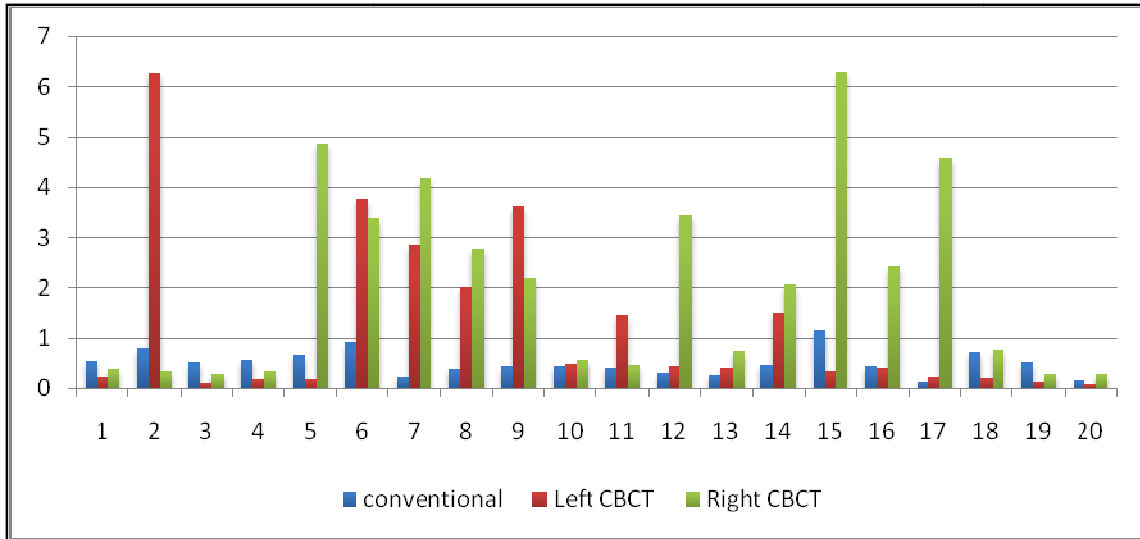


Figure 12. Nasion identification when Sella is the origin of matrix, DEO variability.

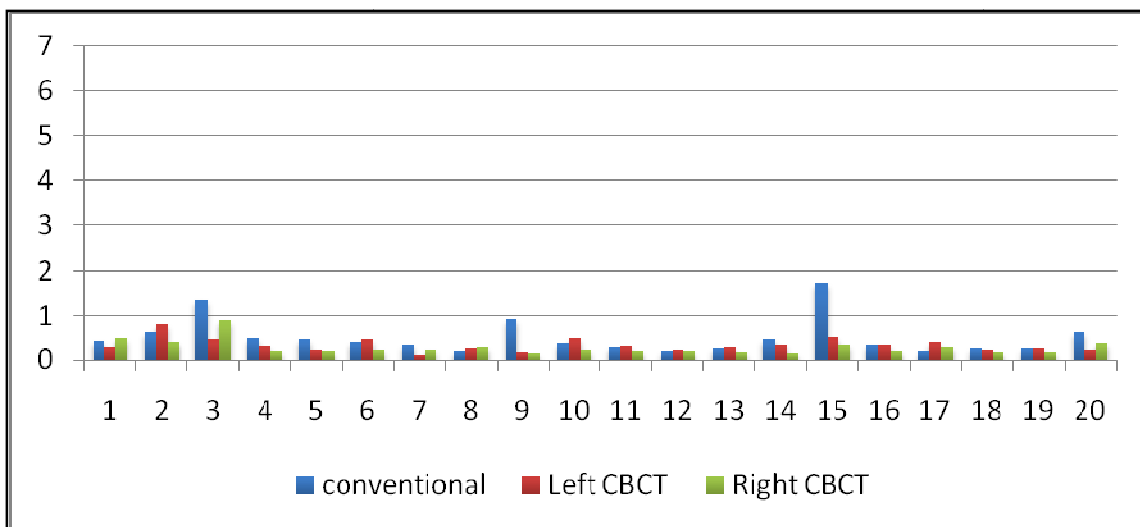


Figure 13. Nasion identification when Sella is replaced by a tick mark on the ruler, DEO variability

Statistically different amounts of variation

Paired comparisons of conventional and CBCT views by landmark and x or y DEO variation is seen in table 7. Statistically significant differences were seen for conventional cephalometric views and CBCT views for Porion, Condylion, Gonion and Orbitale. Table 8 depicts paired comparisons of Right, Left, and MPR CBCT views. No landmark was

significantly different for all comparisons. Gonion and Porion were significantly different in Right and Left CBCT comparisons. Orbitale and Nasion were also significantly different for Right CBCT and MPR comparisons. In addition Orbitale, was significantly different for Left CBCT and MPR comparisons.

Table 7. Paired comparisons of DEO landmark variation for Conventional and CBCT views by Landmark for x and y deviations

DEO Landmarks	Right CBCT-Conventional			Left CBCT-Conventional			MPR- Conventional					
	x diff	p-value	y diff	p-value	x diff	y diff	p-value	x diff	y diff	p-value		
<i>A point</i>	-0.05	0.8606	-0.14	0.593	-0.26	0.3578	-0.2	0.4713	-0.72	0.038	-0.6	0.0044
<i>ANS</i>	-0.52	0.0559	-0.16	0.4665	-0.35	0.059	-0.29	0.1436	-0.91	0.0033	-0.74	0.0063
<i>B point</i>	-0.84	0.0119	-0.29	0.1538	-0.99	0.0049	-0.27	0.2258	-1.06	0.0078	-0.57	0.0342
<i>Condition</i>	-0.92	0.0002	-1.42	0.0001	-1.29	<0.001	-1.76	<0.001	-1.63	<0.001	-2.21	<0.001
<i>Gnathion</i>	-1.19	0.0039	-0.5	0.0063	-1.42	0.0013	-0.45	0.0367	-1.16	0.0186	-0.38	0.1938
<i>Gonion</i>	-2.38	<0.001	-1.09	0.009	-2.97	<0.001	-1.35	0.0039	-2.76	<0.001	-1.01	0.0164
<i>Labraleinferius</i>	-0.68	0.0061	-0.4	0.0096	-0.34	0.157	-0.31	0.0936	-0.79	0.0109	-0.54	0.0098
<i>Labralesuperius</i>	-0.66	0.0025	-0.32	0.0307	-0.33	0.1393	-0.25	0.1468	-0.61	0.0279	-0.36	0.1097
<i>Lower stomion</i>	-0.83	0.0111	-0.2	0.3558	-1.07	0.0007	-0.12	0.6233	-1.28	0.0013	-0.36	0.0934
<i>Mand Inc Tip</i>	-0.66	0.0308	-0.34	0.0167	-0.76	0.009	-0.2	0.1949	-1.15	0.0023	-0.59	0.0052
<i>Max Inc Tip</i>	-0.8	0.0055	-0.24	0.0238	-0.84	0.0021	-0.12	0.4441	-0.57	0.3023	-0.16	0.5431
<i>Menton</i>	-1.2	0.0075	-0.49	0.0106	-1.42	0.0016	-0.25	0.2625	-1.57	0.0051	-0.45	0.0987
<i>Nasion</i>	-0.41	0.0058	-0.05	0.0028	-0.31	0.0512	-0.04	0.0401	0.03	0.9196	0.38	0.0014
<i>Orbitale</i>	-1.85	<0.001	-1.41	<0.001	-1.8	<0.001	-1.3	<0.001	-0.45	0.2679	-0.94	0.0062
<i>Pogomion</i>	-1.01	0.002	-0.47	0.0498	-1.1	0.0011	-0.71	0.0126	-1.22	0.003	-0.57	0.1553
<i>Porion</i>	-2.55	<0.001	-2.18	<0.001	-3.06	<0.001	-3.09	<0.001	-1.54	0.0141	-1.24	0.0585
<i>ST A point</i>	-0.45	0.0325	-0.29	0.1635	-0.34	0.0934	-0.1	0.6874	-0.68	0.0178	-0.3	0.2558
<i>ST B point</i>	-0.84	0.0025	-0.68	0.0117	-0.49	0.0834	-0.6	0.0117	-0.9	0.0107	-1.09	0.0023
<i>ST Gnathion</i>	-1.07	0.0112	-0.54	0.0679	-0.94	0.0515	-1	0.012	-0.89	0.1067	-1.16	0.0117
<i>ST Nasal tip</i>	-0.31	0.0219	-0.31	0.0014	-0.06	0.7798	0.17	0.3801	-0.11	0.6817	-0.07	0.7788
<i>ST Pogomion</i>	-0.82	0.0738	-0.51	0.1735	-0.68	0.0664	-0.74	0.0843	-0.89	0.0281	-0.79	0.1049
<i>Subnasale</i>	-0.52	0.008	-0.26	0.1772	-0.19	0.1839	0.05	0.8307	-0.28	0.2744	0.12	0.7132
<i>Upper stomion</i>	-0.51	0.1119	-0.18	0.1268	-0.62	0.0359	-0.1	0.4698	-0.71	0.036	-0.29	0.0339

■ = statistical significance at Bonferroni corrected alpha of 0.00036 for either x or y component of variation

Table 8. Paired comparisons of DEO landmark variation for CBCT views by Landmark for x and y deviations

DEO	Right CBCT-Left CBCT				MPR- Right CBCT				MPR- Left CBCT			
	x diff	p-value	y diff	p-value	x diff	p-value	y diff	p-value	x diff	p-value	y diff	p-value
<i>A point</i>	0.22	0.2323	0.05	0.8221	-0.68	0.0062	-0.45	0.0243	-0.46	0.0432	-0.4	0.0544
<i>ANS</i>	-0.16	0.4466	0.12	0.6065	-0.4	0.084	-0.58	0.0022	-0.56	0.0454	-0.46	0.1007
<i>B point</i>	0.16	0.2226	-0.02	0.9154	-0.23	0.2353	-0.29	0.1289	-0.07	0.6627	-0.3	0.0764
<i>Condylion</i>	0.37	0.0245	0.34	0.1392	-0.71	0.0044	-0.79	0.0049	-0.34	0.0588	-0.45	0.0635
<i>Gnathion</i>	0.24	0.1076	-0.05	0.716	0.03	0.8542	0.12	0.6078	0.27	0.2118	0.07	0.7432
<i>Gonion</i>	0.58	0.0003	0.26	0.1669	-0.37	0.2419	0.08	0.8077	0.21	0.425	0.34	0.2536
<i>Labraleinferus</i>	-0.34	0.0413	-0.1	0.4454	-0.11	0.4627	-0.14	0.4459	-0.45	0.0094	-0.23	0.1684
<i>Labralesuperius</i>	-0.34	0.0438	-0.07	0.5833	0.05	0.7736	-0.04	0.8385	-0.28	0.1683	-0.11	0.4795
<i>Lower stomion</i>	0.24	0.219	-0.08	0.6839	-0.45	0.0936	-0.16	0.3568	-0.21	0.3424	-0.23	0.1757
<i>Mand Inc Tip</i>	0.1	0.4891	-0.15	0.1521	-0.49	0.0232	-0.25	0.1264	-0.39	0.048	-0.39	0.0106
<i>Max Inc Tip</i>	0.04	0.7797	-0.12	0.2772	0.23	0.5679	0.09	0.6819	0.27	0.539	-0.04	0.8641
<i>Menton</i>	0.22	0.2187	-0.25	0.0473	-0.37	0.1638	0.05	0.7754	-0.15	0.5952	-0.2	0.2753
<i>Nasion</i>	-0.1	0.1769	-0.02	0.0464	0.44	0.0517	0.43	0.0003	0.33	0.1378	0.41	0.0006
<i>Orbitale</i>	-0.05	0.6663	-0.11	0.2298	1.4	<.0001	0.47	0.0667	1.35	<.0001	0.36	0.1536
<i>Pogonion</i>	0.09	0.5827	0.24	0.1219	-0.22	0.1386	-0.1	0.7124	-0.13	0.5823	0.15	0.5112
<i>Porion</i>	0.51	0.0029	0.92	<.0001	1.01	0.0202	0.94	0.0625	1.52	0.0034	1.85	0.0007
<i>ST A point</i>	-0.11	0.3625	-0.19	0.2749	-0.23	0.2253	-0.01	0.9772	-0.34	0.1026	-0.2	0.3713
<i>ST B point</i>	-0.34	0.0835	-0.08	0.6879	-0.07	0.7849	-0.41	0.1383	-0.41	0.0346	-0.49	0.0805
<i>ST Gnathion</i>	-0.14	0.5232	0.46	0.0288	0.19	0.4867	-0.62	0.0252	0.05	0.8773	-0.16	0.6303
<i>ST Nasal tip</i>	-0.25	0.1696	-0.48	0.0165	0.21	0.2014	0.24	0.2135	-0.05	0.8253	-0.24	0.325
<i>ST Pogonion</i>	-0.15	0.5105	0.23	0.4836	-0.07	0.814	-0.27	0.4656	-0.22	0.4048	-0.04	0.8872
<i>Subnasale</i>	-0.33	0.0135	-0.3	0.0691	0.24	0.1246	0.38	0.2058	-0.09	0.6934	0.08	0.7911
<i>Upper stomion</i>	0.11	0.4466	-0.08	0.5028	-0.2	0.4007	-0.11	0.5019	-0.09	0.6622	-0.2	0.2623

■ = statistical significance at Bonferroni corrected alpha of 0.00036 for either x or y component of variation

Table 9. x and y landmark identification variability by modality

Modality	Conventional Ceph	Left half CBCT Ceph	Right half CBCT Ceph	MPR view
X DEO	2.34	1.19	1.31	1.15
Std dev	0.90	0.38	0.45	0.56
Y DEO	1.94	1.59	1.59	1.49
Std dev	1.02	0.75	0.75	0.82

DISCUSSION

Conventional cephalograms are considered a valuable tool for diagnosis and treatment planning of dento-facial disharmonies but are well known for their limitations including: errors in patient position, differential magnification of bilateral structures and superimposition of craniofacial structures. (Midtgard et al., 1974; Houston, 1983). The results of this study show that landmark identification for conventional cephalograms produced statistically greater variability when compared with each of the alternative CBCT modalities (Tables 4-9). Rejection of the null hypothesis of no difference between conventional cephalometric imaging and alternative CBCT views is not surprising given our initial supposition that increased variability is a function of structure noise from the superimposition of bilateral structures in conventional cephalograms. This was borne out by the fact that x variation was greater than y variation for conventional cephalograms; this pattern was reversed with y variation being greater than x for CBCT modalities for Condylion, Gonion, Orbitale and Porion (Table 9). These findings are consistent with previous studies that demonstrated that overlapping of bilateral structures resulted in a point intermediate between the two outlines, introducing errors in landmark localization (Hurst et al., 2007).

Cephalometric relationships are frequently described relative to reference planes such as the Frankfort horizontal plane, the natural head position or sella-nasion (Hurst et al., 2007). In this study natural head position was the plane of orientation used for conventional cephalograms. Although 3D measurements of CBCT volumes are free from the influence of patient position during image acquisition, the orientation of the secondary reconstruction of the volume directly impacts the projection of anatomy in synthesized 2D cephalometric views. Unlike errors in skull position seen in conventional cephalometric images due to faulty positioning of the cephalostat or faulty positioning of the patient within the cephalostat, orientation of the CT volume can be corrected by iterative adjustment and reassessment. The alignment of the transporionic axis to orient the midsagittal plane was used in the 3D modalities to simulate the plane of orientation used in conventional cephalograms. Orientation of Frankfort plane horizontal, while potentially different from natural head position, permitted standardization of cases. Rotation of the midsagittal plane should have no impact on landmark identification as this is analogous to small rotations of the monitor or the observer's head while viewing an image. Reorientation of the measurement matrix because of changes in Frankfort plane will make a difference in the distribution of x and y components of the variation that is measured; however, these differences are estimated to be less than 1.5% for angular changes up to 10° in the Frankfort plane ($\cosine\ 10^\circ = 0.985$).

The results of this study show that no landmark was significantly different across all CBCT modalities. However, Orbitale displayed significantly less variation in Right and Left CBCT in comparison with MPR. This variation was significant in the antero-posterior direction but not in the cranio-caudal direction. This may be related to observers

selecting different medio-lateral positions on the orbital margin that, while at the same vertical height, were at varying anterior-posterior positions as a result of the posterior rotation of the lateral aspect of the maxillary surface. Significantly less variation is also seen in Right CBCT identification of Nasion in comparison with MPR views. Although not statistically significant, a similar trend of reduced variation in landmark identification is seen for Left CBCT views. No easy explanation for this observation can be provided. However, the difference in variation between modalities was well short of clinical significance ($DEO < 0.5 \text{ mm}$). Left CBCT exhibited significantly less variability for Porion and Gonion identification than Right CBCT. No reason for this discrepancy is readily apparent (Table 8).

While the focus of this study was to explore differences in precision between modalities, it is useful to comment on landmark variability across modalities. In general variability in the vertical dimension for all modalities was consistently high for soft tissue pogonion (Figure 9-11). Many of the subjects included in our sample exhibit Class II skeletal profiles with receding chin lines. In the absence of a chin prominence, pogonion is located on a slope. Greater variation between observers might be expected in this situation.

When the clinical significance of landmark localization is considered it can be seen that for conventional cephalograms over half of the landmarks investigated in this study exceeded a 2 mm variability threshold when as measured by DEO. This was reduced to one or two landmarks for CBCT alternatives.

The results of this study show that although MPR is a dynamic technique offering the possibility of visualizing a landmark in three right angle views (sagittal, coronal, axial) it has limitations. These may be related to an imprecise landmark definition or difficulty in extending a 2D definition to a 3D modality, creating more variability among observers (Figure 6). An example of this is Porion where some observers localized this structure in the soft tissues of the ear canal whereas others localized it on a bone/soft tissue margin. Another limitation of MPR views was the introduction of error by the observers during the digitizing process where landmarks could be misplaced if the identification order was not carefully followed. Unlike the software for recording 2D modalities which listed each landmark by name, the MPR software only provided a numerical order which the observer had to correlate with a printed list of landmarks. When discovered, this problem was corrected by having the observer redo the entire sequence of landmark localization for the faulty case. This is a problem that can be overcome by replacing the generic list with named landmarks in a logical sequence.

Sella is an important landmark from the perspective of Orthodontic diagnosis and treatment planning. It was particularly important in this study because the 2D cephalometric tracing software utilizes this point as the origin of the matrix on which all other landmarks are identified. An error in locating Sella is propagated through all other landmarks. In our study a total of 7 cases in the right and left half CBCT cephs presented difficulty in visualization of the Sella structure. In the initial assessment of landmark variability it was noted that some cases produced variability in excess of 10 mm due to variation in the location of Sella. It was found that inadequate orientation on the midsagittal plane of the volume prior to the generation of the radiographs was related to

the difficulty on the depiction of this point. Therefore, to remove spurious variability from other landmarks it was decided to replace Sella with the identification of a tick mark at the 120 mm point of the ruler on the half CBCT cephs and at the 10 mm tick mark on midsagittal plane ruler in the conventional cephalogram. Variability in locating Sella can be reduced by constructing a half volume that extends just beyond the midsagittal plane. This anecdotal finding and its influence on precision of location of other midline landmarks needs to be confirmed with further study.

While Sella was problematic for establishing the origin a measurement matrix, Nasion appeared to be a precise landmark for all modalities (Figures 4-7). The results of this study shows that when Sella was used as the origin for the x, y matrix, Nasion presented a high variability for Right and Left CBCT views when compared with conventional cephalogram (Figure 12). Once the origin of the matrix was relocated to a tick mark on a ruler, Nasion data provided reduced variability for Right and Left CBCT views while conventional cephalograms precision remained the same (Figure 13). Based on these results, Nasion could serve as a matrix anchor point for computer based cephalometric image assessment. Points that are most reliable in a 3D coordinate system require additional research. Such points will require operational definitions that describe the point's appearance in the 3rd dimension.

Specific reference points and presumed bilateral symmetry become problematic when these factors are abnormal. In this study, the sample was composed of pre-treated orthodontic surgical patients. Although inclusion criteria were not based on symmetry, many of our subjects were asymmetric. While new methods of 3D assessment are under development, the results of this study suggest that CBCT modalities permit more precise

landmark identification than conventional cephalograms and may be applied in clinical situations where precision of landmark identification is required. Additional studies are needed to evaluate the precision of landmark localization and the cephalometric assessment of CBCT half skull projections compared to conventional views and the impact of differences on diagnosis and treatment planning for populations of symmetric and asymmetric patients.

A number of factors must be considered in choosing a radiographic examination. These include the probability of obtaining the diagnostic information that is sought from the examination, the cost of the examination, and the risks of the examination. These must be weighed against the same factors for alternate diagnostic procedures as well as the value of the information that is sought and the risks and costs of inadequate diagnosis. Standard orthodontic diagnosis often employs panoramic, lateral cephalometric and PA cephalometric radiography. Estimated risk from these 3 examinations using ICRP Recommendations for calculating effective dose is between 25 and 35 μSv (Ludlow et al. in press) Alternate CBCT doses from a single large FOV scan that is useful for complete orthodontic diagnosis range from 68 to 1073 μSv (Ludlow et al. in press 2). The excess risk, depending on the radiographic device, is equivalent to a few days to several weeks of average US per capita background dose. If the diagnostic information provided by the CBCT scan improves treatment results, shortens treatment time, or reduces treatment cost, this increased risk may be worthwhile. In the absence of such a benefit the technique cannot be recommended. Future study of the impact of CBCT diagnostics on patient treatment is needed.

CONCLUSIONS

- Conventional cephalogram images produce more variability in landmark identification compared with CBCT modalities.
- CBCT projections provide significantly more precise location of Condylion, Gonion, Orbitale, and Porion landmarks overcoming the problem of superimposition of these bilateral landmarks seen in conventional cephalograms.
- The potential for more precise location of landmarks in the three planes, sagittal, coronal and axial MPR images was not demonstrated in this study. While overall performance of MPR views was not different from Right and Left CBCT cephalometric views, Nasion and Orbitale identification were significantly more variable in MPR views. This may be due to the absence of a clear definition of these landmarks in the 3rd (medial-lateral) dimension.
- Three dimensional landmark identification requires suitable operational definitions of the landmark location in each of the three planes of the space.
- CBCT cephalometric image reconstruction can be recommended as an alternative to cephalograms when CBCT volume is already available, thus reducing additional x-ray exposure and examination expense.

REFERENCES

- Cohnen M, Kemper J, Mobes O, Pawelzik J, Modder U. Radiation dose in dental radiology. *Eur Radiol.* 2002; 12(3):634-7.
- Hideki K, Koichi Y, Hideki K, Kazuhide K, Takasashi N. Standardization of 3-D CT measurements for length and angles by matrix transformation in the 3-D coordinate system. *Cleft Palate Craniofacial Journal.* 2000; 37:349-56.
- Honda K, Arai Y, Kashima M, Takano Y, Sawada K, Ejima K. Evaluation of the usefulness of the limited cone-beam CT (3DX) in the assessment of the thickness of the roof of the glenoid fossa of the temporomandibular joint. *Dentomaxillofacial Radiology.* 2004; 33(6):391-5.
- Honda K, Matumoto K, Kashima M, Takano Y, Kawashima S, Arai Y. Single air contrast arthrography for temporomandibular joint disorder using limited cone beam computed tomography for dental use. *Dentomaxillofacial Radiology.* 2004; 33(4):271-3.
- Houston WJ. The analysis of errors in orthodontic measurements. *Am J Orthod.* 1983; 83:382-90.
- <http://www.qrverona.it/imagelink/NTTRIALBETA1.pdf>.
- Hurst CA, Eppley BL, Havlik RJ, Sadove AM. Surgical cephalometrics: applications and developments. *Plastic Reconstructive Surgery.* 2007; 120(6):92e-104e.
- Kumar V, Ludlow J, Cevidanes LHS, Mol A (2008). In vivo comparison of conventional and cone beam CT synthesized cephalograms. *Angle Orthodontist*, 78:5:873-879
- Ludlow JB, Brooks SL, Davies-Ludlow LE, Howerton B. Dosimetry of 3 CBCT units for Oral and Maxillofacial Radiology. *Dentomaxillofacial Radiology.* 2006; 35: 219-226
- Ludlow JB, Davies-Ludlow LE, Brooks SL. Dosimetry of two extraoral direct digital imaging devices: NewTom cone beam CT and Orthophos Plus DS panoramic unit. *Dentomaxillofacial Radiology.* 2003; 32(4) 229-34.
- Ludlow JB, Ivanovic M. Comparative Dosimetry of Dental CBCT Devices and 64 row CT for Oral and Maxillofacial Radiology in press *Oral Surg Oral Med Oral Pathol Oral Radiol Endodont* 3/13/2008.
- Ludlow JB, Davies-Ludlow LE, White SC. Patient risk from common dental radiographic examinations. In press *Am Dent Assoc J* 3/26/08 manuscript ID 099-08*

- Midtgard J, Bjork G, Linder-Aronson S. Reproducibility of cephalometric landmarks and errors of measurements of cephalometric cranial distances. *Angle Orthod.* 1974; 44:56-61.
- Ngan DC, Kharbanda OP, Geenty JP, Darendeliler MA. Comparison of radiation levels from computed tomography and conventional dental radiographs. *AustOrthod J.*2003; 19(2):67-75.
- Papadopoulos M, Jannowitz C, Boettcher P, Henke J, Stolla R, Zeilhofer H, Kovacs L, Erharadt W, Biemer E, Papadopoulos N. Three-dimensional fetal cephalometry: An evaluation of the reliability of cephalometric measurements based on three-dimensional CT reconstructions and on dry skulls of sheep fetuses. *Journal of Cranio-Maxillofacial Surgery.* 2000; 33:229-237.
- Por Y-C, Barcelo CR, Sng K, Genecov D, Salyer K. A novel method for measuring and monitoring monobloc distraction osteogenesis using three dimensional computed tomography rendered images with the “Biporion-Dorsum Sellae” plane. Part I: Precision and reproducibility. *The Journal of Craniofacial Surgery.* 2005; 16:430-435.
- Scarfe W, Farman A, Sukovic P. Clinical applications of Cone-Beam Computed Tomography in dental practice. *JCDA.* 2006; 72:75-80.
- Schulze D, Heiland M, Thurmann H, Adam G. Radiation exposure during midfacial imaging using 4 –slice and 16-slice computed tomography, cone beam computed tomography systems and conventional radiography. *Dentomaxillofacial Radiology.* 2004; 33(2):83-8.
- Tsiklakis K, Syriopoulos K, Stamatakis HC. Radiographic examination of the temporomandibular joint using cone beam computed tomography. *Dentomaxillofacial Radiology.* 2004; 33(4):196-201.